Journal of Iron and Steel Research, International 24 (2017) 561—568

Contents lists available at ScienceDirect

Journal of Iron and Steel Research, International

journal homepage: www.chinamet.cn

Effect of Si on high temperature oxidation of 30Cr13 stainless steel

Hong-huan Mao, Xing Qi, Jing Cao, Li-cong An, Yi-tao Yang*
School of Materials Science and Engineering, Shanghai University, Shanghai 200072, China

ARTICLE INFO

Key words:
Metallic material
Martensitic stainless steel
High temperature oxidation
Oxidation kinetics

ABSTRACT

The effect of Si on the high temperature oxidation behavior of the 30Cr13 martensitic stainless steels was investigated. The underlying mechanism was further discussed by oxidation kinetics curves, scanning electron microscopy (SEM) and X-ray diffraction (XRD) analysis. It was observed that the addition of Si can significantly reduce the mass gain per unit area and the oxidation rate of the experimental steels. With the increase of Si content, the film surface composed of the wheat-like oxides turned into the small granular oxides after oxidation for 120 h. The SiO_2 film formed on the metal substrate inhibited the outward diffusion of the metal cation and the inward diffusion of the oxygen anion; thus, the high temperature oxidation resistance was enhanced.

1. Introduction

13 wt. % Cr-type stainless steels are most widely applied to machinery manufacturing[1]. 30Cr13 martensitic stainless steel has relatively high carbon content and possesses excellent mechanical properties and good corrosion resistance, thus making it widely applied in the aerospace, medical and machinery manufacturing[2]. As the first-designed superalloy, Cr-type iron-base superalloy has been widely investigated and rapidly developed. However, with the rapid progress in science and technology, there are more and more requirements for material performance, and never will it meet the need of modern society. In the 1920s, Michael Farada, an outstanding Britain physicist, investigated the influences of alloying element on the steel properties, showing that alloying can directly affect the oxidation resistance of stainless steel. Huang and Yang[3] explored the effects of Nb and Ti on 430 stainless steel, and found that oxidation activation energy of material was significantly decreased, and the oxidation resistance got improved in consequence. Fujikawa et al.[4] added 0.03 wt. % Y into 19Cr-10Ni-1.5Si; the results indicated that Y could isolate oxide, in which the process of cation outward diffusion was suppressed, and make Si in the inner layer oxidize faster. Addition of Si into stainless steel is a common method to improve high temperature oxidation resistance. Many researchers indicated that small increase of Si content has a beneficial effect on oxidation resistance, because Si could be passivated and form silica film to increase the oxidation resistance of the high Cr iron-base superalloy[5-8]. Compared to Cr, Si is of higher oxygen affinity, forming SiO_2 oxide film between Cr_2O_3 oxide film and matrix in alloy; thus, outward diffusion of Cr ions in the matrix becomes more difficult, and a better oxidation resistance of alloy is achieved accordingly[9-13]. Hence, researchers have paid extensive attention to Cr-Si type iron-base alloys. In this paper, based on 30Cr13 martensitic stainless steels with different amounts of Si addition, the micrograph, chemical composition, and phase constitution of materials after oxidation at 900 ℃ were analyzed, and the mechanism of high temperature oxidation resistance was further studied, so as to provide certain theoretical basis for practical production.

2. Experimental

In this work, 30Cr13 martensitic stainless steels were melted in a high vacuum electric furnace. The chemical compositions of alloys were analyzed by PMI-MASTER PRO, as shown in Table 1. The experimental alloys were marked as Si0.5 to Si2.5 with increasing the silicon content.

After samples were melted into ingots, heat treatments were taken to improve the mechanical proper-

* Corresponding author. Prof., Ph.D.; Tel.: +86-21-56334465.
E-mail address: *yyt@staff.shu.edu.cn* (*Y. T. Yang*).

Received 24 July 2016; Received in revised form 6 December 2016; Accepted 19 December 2016
Available online 15 May 2017

Table 1
Chemical composition of test material (mass%)

Material No.	C	Si	Mn	Cr	Fe
Si0.5	0.305	0.48	0.429	14.0	Balance
Si1.0	0.298	1.07	0.418	13.7	Balance
Si1.2	0.295	1.22	0.403	13.2	Balance
Si1.4	0.319	1.42	0.420	13.1	Balance
Si1.5	0.296	1.54	0.416	13.5	Balance
Si2.5	0.278	2.48	0.395	12.9	Balance

ties. In order to reduce composition segregation, the alloys were diffusion annealed at 1200 ℃ for 2 h, then austenitized at 950 ℃ for 30 min, followed by air cooling. After quenching, the samples were tempered at 250 ℃ for 2 h. Samples of 10 mm×10 mm×3 mm were cut from ingots using wire cut electrical discharge machining (WEDM), then milled to the roughness value below 0.8 μm. A final rinse in ethanol was carried out before oxidation treatment.

The oxidation experiments were conducted in a chamber electric furnace (YFA12/15G-Y) with some small holes where air flows freely. 6 sets of samples were oxidized respectively at the same temperature of 900 ℃ for 5, 10, 20, 40, 80 and 120 h, then air cooled to room temperature in the airtight crucibles. Aiming to compare the mass gain per unit area after oxidation and evaluate their oxidation behavior, an electronic analytical balance with precision of 0.0001 g was used.

Microstructure of oxidized surface and cross section of each experimental specimen was observed using HITACHI SU-1500, and the oxides in the surface were analyzed by energy-dispersive X-ray spectrometry (EDS). X-ray diffraction (XRD) analyses were carried out on a 18KW D/MAX2500V+/PC. The oxidation specimen was mounted in epoxy resin, then ground with aluminum oxide water proof abrasive papers from 400 to 1200 grit for further cross section observation.

3. Results and Discussion

3.1. High temperature oxidation macromorphology and kinetic analysis

Observations for different samples oxidized at 900 ℃ for different time reveal that the surface of alloys with Si contents of 0.5%, 1.0% and 1.2% oxidized beyond 20 h becomes coarse and irregular, and some parts of the oxidation layer are warped and cracked, even separated from the matrix, which loses protection completely. As shown in Fig. 1(a), the morphology of oxidation film on sample oxidized for 80 h is more smooth and dense, while that of sample oxidized for 120 h (Fig. 1(b)) becomes more coarse. However, alloys with Si content of 1.5% performs good oxidation resistance before 80 h, but also gets coarse after oxidation for 120 h; cracks were not shown. As for alloys with Si contents of 1.5% and 2.5%, when oxidation time comes to 120 h, the oxidation surface is still smooth, which plays a vital role in protecting the inner matrix.

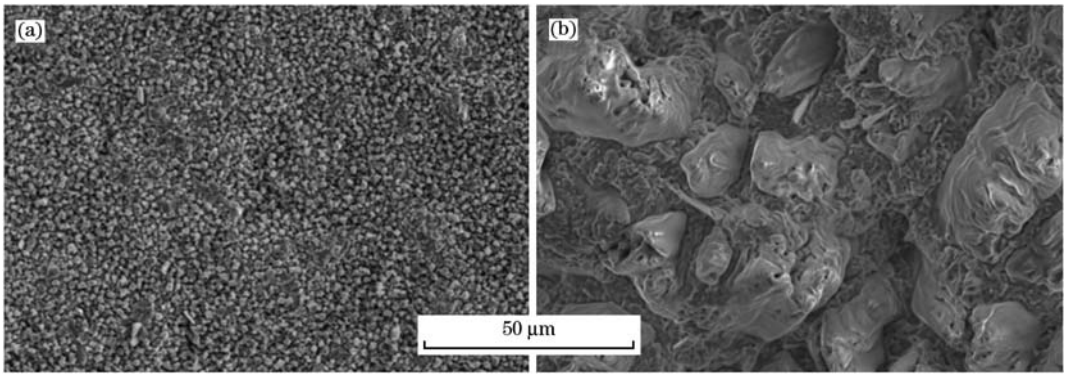

Fig. 1. Morphology of 1.4% Si alloy after oxidation for 80 h (a) and 120 h (b).

According to the mass gain per unit area during the oxidation, the oxidation kinetics curves presented in Fig. 2 show that the mass gain per unit area of all alloys increases with the oxidation time, and Si0.5, Si1.0, and Si1.2 reveal a similar oxidation behavior, which changes significantly and has a higher mass gain, while Si1.4 displays a rapid growth in the mass gain from 80 to 120 h, and Si1.5 presents a relatively flat curves, with almost the same mass gain during the experiment. After oxidation for 120 h, the mass gain of Si2.5 is only 0.64 mg, which is the smallest of all alloys. Except for Si1.4, the other alloys mass gain all show a parabolic growth trend in the first 20 h; then the increase becomes even and the oxidation rates decrease, which reveals that the steady states are reached. Through comparing the oxidation kinetics curves of six alloys, it can be concluded that during the oxidation, alloys might experience three different stages: (1) Firstly, a compact thin oxidation layer with better oxidation resistance was formed; (2) Then, some new oxides which have bad oxidation resistance were

generated on the dense oxidation layer, making oxidation rate become faster; (3) A new oxidation layer was formed above the former one, and when reaching a certain thickness, the layer gets steady. In addition, Si0.5, Si1.0 and Si1.2 all come to stage 3, while Si1.4 was between stages 2 and 3, and Si1.5 and Si2.5 were still in stage 1. In conclusion, in the same condition, Si2.5 has the least mass gain and the best oxidation resistance.

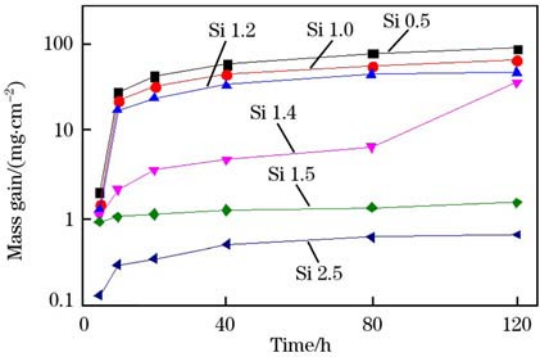

Fig. 2. Oxidation kinetics curves at Si0.5, Si1.0, Si1.2, Si1.4, Si1.5 and Si2.5.

The thicknesses of oxidation layer of six alloys were measured by scanning electron microscopy (SEM) and are summarized in Fig. 3. The results indicate that the thickness of oxidation layer decreases with the Si content; Si0.5 and Si1.0 have thicker oxidation layers of 650 and 500 μm respectively, while oxidation layers of Si1.5 and Si2.5 were both thinner than 10 μm. Mougin et al. [14] studied 18Cr stainless steels and their results demonstrated that the thickening of oxidation layers might make the adhesive ability between matrix and oxidation layer decrease exponentially, which dramatically weaken the adhesive strength between the two layers.

Based on the research made by Li[15], when oxidation kinetics curves of metallic materials obey parabolic law, the kinetics should fit the following formula.

$$\Delta m^n = k_p t \quad (1)$$

where, Δm is the mass gain per unit area, (mg · cm^{-2}); n and t are the index and oxidation time respectively; and k_p represents oxidation rate constant, (mg · cm^{-2} · h^{-1}). In order to obtain the k_p of six alloys under the same condition, the curves shown in Fig. 1 were nonlinearly fitted to Eq. (1). Table 2 shows the results of the obtained oxidation rate constants. It can be concluded that when Si content increases, k_p gradually decreases. Si0.5, Si1.0 and Si1.2 have bigger k_p, which illustrates that the growth rate of oxidation film is higher and the oxidation layer becomes thicker, so that the matrix was destroyed significantly. Compared to the alloys with lower Si content, k_p of Si1.5 and Si2.5 sharply decreases, especially for Si2.5, the value is only 2.98×10^{-3} mg · cm^{-2} · h^{-1}, which is several orders of magnitude smaller than those of other alloys, and thus the alloy possesses excellent oxidation resistance. Therefore, the addition of Si can dramatically decrease k_p, then slow down the growth rate of oxidation film, which effectively protects the inner materials, that is why the high temperature oxidation resistance of alloys was improved.

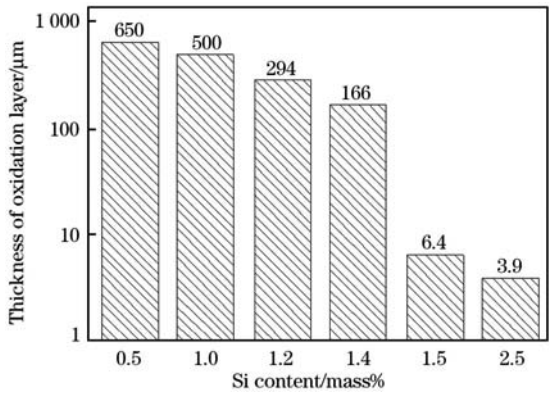

Fig. 3. Thickness of oxide layer oxidized at 900 ℃ for 120 h.

Table 2
k_p of six samples at 900 ℃ (mg · cm^{-2} · h^{-1})

Si0.5	Si1.0	Si1.2	Si1.4	Si1.5	Si2.5
51.46	7.69	4.42	1.28	0.10	2.98×10^{-3}

3.2. Surface morphology and composition of oxidation film

It is generally believed that the morphology of oxidation film could determine whether the high temperature oxidation resistance is good or bad. An uniform oxidation film with a smooth and compact structure and within fine oxide particles preforms better at high temperature; otherwise, it has worse oxidation resistance[16]. Fig. 4 displays the SEM surface morphologies of six alloys oxidized for 120 h at 900 ℃. The corresponding composition analyses are shown in Fig. 5. As shown in Fig. 4, there are large differences in surface oxidation film among different alloys. The oxidation films of Si0.5, Si1.0, Si1.2 and Si1.4 are rough and coarse, whereas those of Si1.5 and Si2.5 are flat, and the oxide particles are finer, which isolates the substrate from the outside environment, protecting the substrate effectively. When oxidized at 900 ℃ after 120 h, the oxide particles of Si0.5 are rather bigger (see Fig. 4(a)), which is about 20 μm. According to the composition analysis via EDS in Fig. 5(a), the oxides consist of Fe and O, but the iron oxides have a loose structure; thus, they cannot prevent oxygen diffusing into the substrate efficiently, making the oxidation film unable to protect the substrate well. In addition, the oxidation film has formed a sintering oxide shell at this

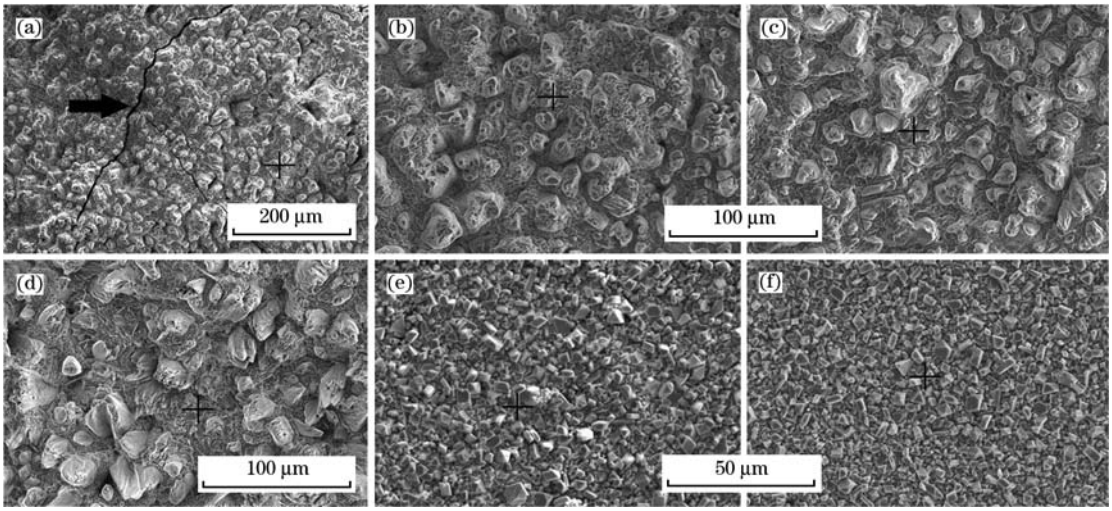

(a) Si0.5; (b) Si1.0; (c) Si1.2; (d) Si1.4; (e) Si1.5; (f) Si2.5.

Fig. 4. SEM images of six samples oxidized at 900 ℃.

stage, and the oxidation layer gets cracked under stress, as indicated by the arrow in Fig. 4(a). The oxidation film of Si1.0 is uneven (Fig. 4(b)), and the sizes of oxides are various. The sizes of larger oxides in the left bottom are approximately 15 μm, while in the right of the figure, the oxides are in powder shape, so the loose structure is difficult to resist oxygen diffusing into the substrate. The oxides in the oxidation film might be composed of iron oxides on the basis of EDS analysis (Fig. 5(b)). As seen in Fig. 4(c,d), the oxidation film morphology is similar to that in Fig. 4(b), and its surface is made up of Fe and O. When Si content comes to 1.5%, there is an obvious change in the surface morphology, as shown in Fig. 4(e). The oxidation film is constituted by fine oxide particles, which are almost in octahedral shape. Furthermore, oxide particles with different sizes are distributed separately; some of them are in the size of 2 μm, and the larger ones are 5 μm. With further analyzing by EDS in Fig. 5(e), it is shown that the granular oxides are made up by O, Cr and Mn. Observing the oxidation film in Fig. 4(f), there are fine and uniform oxide particles in it, and contrasted with the oxidation film of Si1.5, there are less large granular oxides; the oxidation film surface is more flat and compact, then benefits the prevention of oxygen inward diffusion. As indicated by EDS, the granular oxides comprise O, Cr, and Mn. Chromium oxides and manganese oxides have smaller size, and the oxides are closely combined with each other. Resulting from this, iron diffuses slowly in these oxides, then the great oxidation resistance is obtained.

Above all, with more amount of Si, the oxides in the surface are changed from larger wheat-like oxides (iron oxides) to finer granular oxides, which are chromium and manganese oxides.

On the ground of observation of the oxidation kinetics curve of Si1.4, its oxidation kinetics behaviors are slightly different from those of the others. To

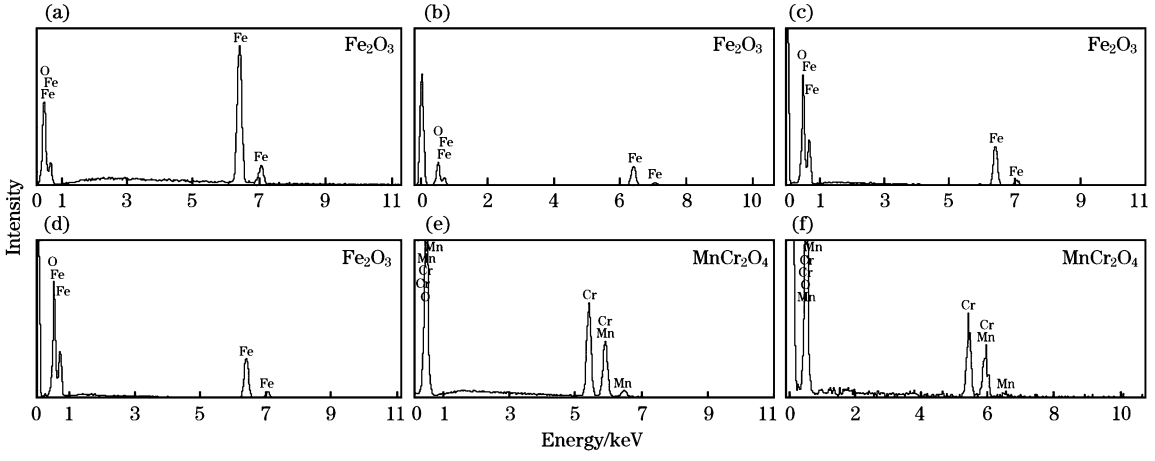

(a) Si0.5; (b) Si1.0; (c) Si1.2; (d) Si1.4; (e) Si1.5; (f) Si2.5.

Fig. 5. EDS spectra of oxides on surface of six samples oxidized at 900 ℃.

investigate the oxidation mechanism, the oxidation films of different oxidation time are observed, as shown in Fig. 6. When oxidized for 20 h, the oxide particles are rather small and generally less than 1 μm (presented in Fig. 6(a)). As oxidation time increases to 40 h, the fine granular oxides in Fig. 6(a) grow up into the shape observed in Fig. 6(b); and some nodular oxides, a kind of oxide that composed of gathered granular oxides, appear and dispersively distribute on the oxidation film. Afterwards, when oxidized for 80 h, the nodular oxides grow up and gather together, forming the island-like oxides displayed in Fig. 6(c). Fig. 6(f) is the further observation of the island-like oxides. The gray matrix oxides comprise lots of granular oxides, whereas the island-like oxides above them have loose structures. The points A and B in Fig. 6(f) are chosen to analyze via EDS and the results are presented in Fig. 6(g, h). By means of EDS, besides chromium oxides and manganese oxides, iron oxides also exist there, and the island-like oxides are completely made up of iron and oxygen.

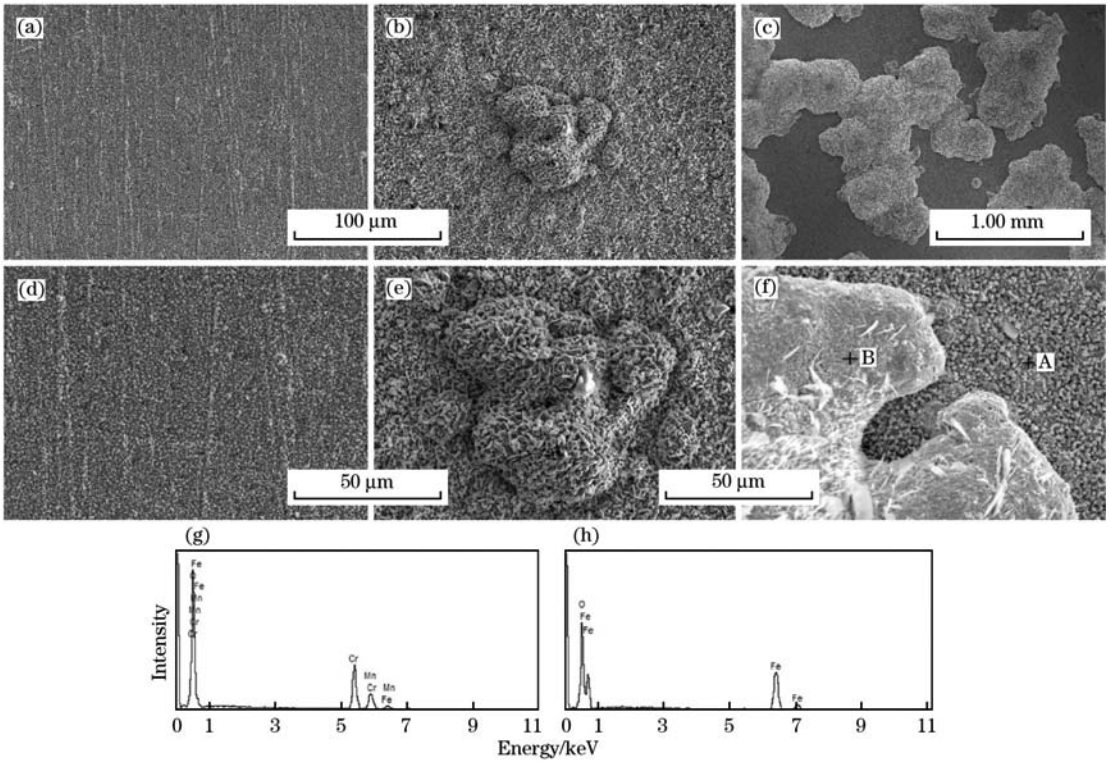

(a), (d) 20 h; (b), (e) 40 h; (c), (f) 80 h; (g) Point A in (f); (h) Point B in (f).

Fig. 6. SEM images of Si1.4 oxidized at 900 ℃.

By analyzing the evolution rules of oxidation of Si1.4, it is revealed that in the early stage, the oxidation film is composed of granular oxides; as oxidation proceeds, the nodular oxides appear on the surface of the flat and compact oxidation film, and then the island-like oxides formed subsequently are dispersively distributed on the oxidation film, and cover it all eventually. In the last stage, wheat-like oxides appear above the island-like oxides till covering the whole oxidation film.

Additionally, the evolution rules are also suitable for other samples. Based on this, it might be concluded that the increasing addition of Si could delay the whole oxidation process. The same phenomenon occurring in Si1.4 would also happen in Si1.5 and Si2.5 in case of continuing to oxidation to certain extent. Apparently, the addition of Si improves the high temperature oxidation resistance of materials effectively.

3.3. Phase analysis of oxidation film

Aiming to further determine the type of oxides, XRD analysis was applied to investigate the oxidized samples, and the results are displayed in Fig. 7.

As illustrated in Fig. 7, only Fe_2O_3 is detected in Si0.5, Si1.0, Si1.2 and Si1.4, demonstrating that the oxidation film surface is composed of iron oxides. But Cr_2O_3, Fe_2O_3 and $MnCr_2O_4$ exist in Si1.5 and Si2.5; meanwhile, the Fe-Cr matrix phase is detected. This is because the detection depth of XRD is about 50 μm, and the metallic substrate could be detected if the oxidation film is thin enough. Otherwise, the phase under the oxidation film could not be detected when the thickness of the oxidation film is more than the detection range of XRD. Combining with the EDS results in Fig. 5, the granular oxides on the oxidation film of Si1.5 and Si2.5 are $MnCr_2O_4$,

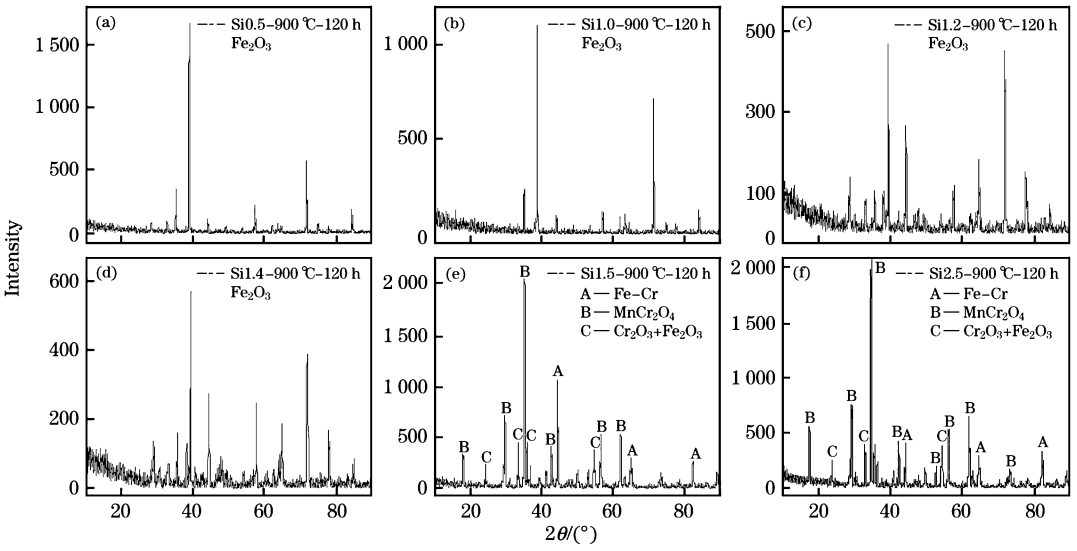

(a) Si0.5; (b) Si1.0; (c) Si1.2; (d) Si1.4; (e) Si1.5; (f) Si2.5.

Fig. 7. XRD spectra of all steels oxidized at 900 ℃ for 120 h.

then Cr_2O_3 and Fe_2O_3 are ought to be under the $MnCr_2O_4$ oxidation film.

3.4. Analysis on cross section of oxidation layer

In order to understand the structure of oxidation layer, the cross section was studied. Fig. 8 presents the SEM morphology of six alloys, and the corresponding line scan analysis is shown in Fig. 9. Clearly, there is evident delamination phenomenon in Si0.5, Si1.0 and Si1.2 after oxidizing at 900 ℃ for 120 h, which reflects the poor oxidation resistance at this stage. Additionally, according to the EDS and XRD analyses, the outmost layer of three alloys is Fe_2O_3; then, the outer layer is composed of Cr_2O_3, $MnCr_2O_4$ and Fe_2O_3; lastly, the inner layer next to the substrate is a layer of discontinuously distributed SiO_2 thin film. The outmost layer of Si0.5 is loose and porous; during the oxidation process, these microspores in the outmost layer tend to grow into cracks, and oxygen could easily diffuse into the substrate and react with it, leading to inner oxidation. Comparing Figs. 8(a) and 8(b), the combination between the oxidation film and the substrate in Si1.0 is worse than that in Si0.5, and this phenomenon conforms to the research made by Bamba et al.[17], which showed that increasing the amount of Si could weaken the attachment energy between the oxidation film and the metallic substrate. Although delamination phenomenon was also found in Si1.4, the EDS results indicated that there is no obvious distinction in chemical composition between inner and outer layer, and oxides are both Cr_2O_3 and Fe_2O_3. However, the structure of the oxidation film of Si1.5 and Si2.5 has a big difference: the outmost layer is the oxidation film formed by granular oxides $MnCr_2O_4$, then a compact Cr_2O_3 oxidation film is found, and SiO_2

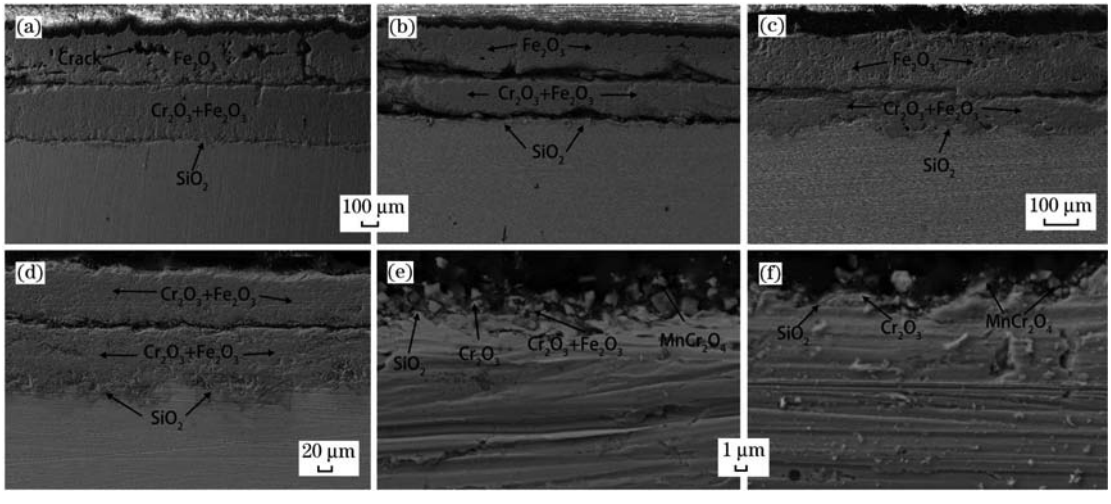

(a) Si0.5; (b) Si1.0; (c) Si1.2; (d) Si1.4; (e) Si1.5; (f) Si2.5.

Fig. 8. SEM images of surface cross-section of all steels oxidized at 900 ℃ for 120 h.

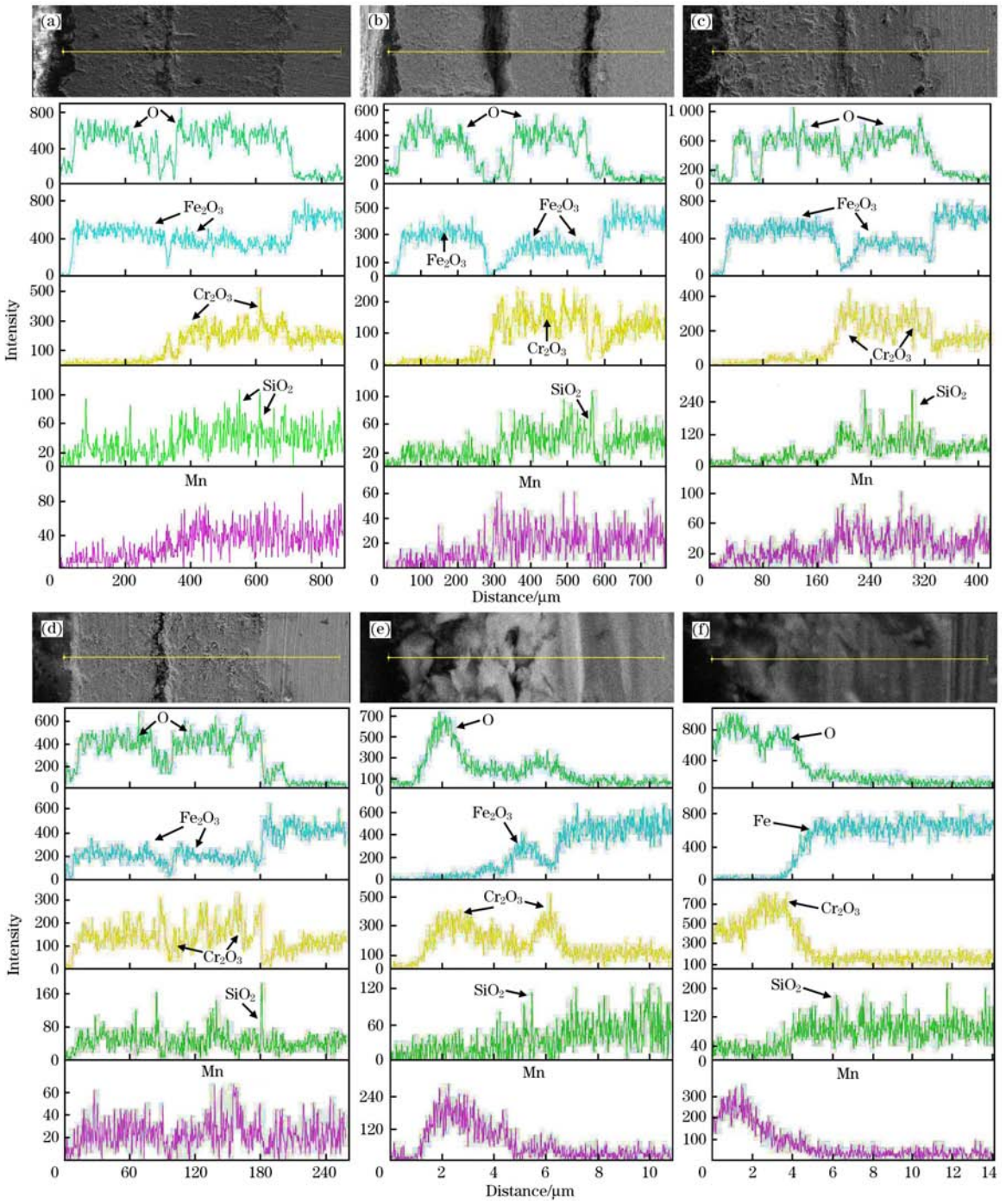

(a) Si0.5; (b) Si1.0; (c) Si1.2; (d) Si1.4; (e) Si1.5; (f) Si2.5.

Fig. 9. EDS spectra of surface cross-section during 120 h at 900 ℃.

film exists between the Cr_2O_3 oxidation film and the metallic substrate.

From the analysis above, the evolution rules of oxidation layer at high temperature in 30Cr13 stainless steel may come to the conclusion that, when oxidized at 900 ℃, due to the strong affinity between Si and O, O firstly reacts with Si, then SiO_2 is formed on the surface of alloys, instead of surrounding by iron oxides. They grow smoothly on the surface of alloys. Hence, SiO_2 is homogeneously distributed on the oxidation film[18]. This kind of compact SiO_2 film could inhibit oxygen anions diffusing inward and metal cations diffusing outward; thus, the substrate could be well protected. Additionally, since Si and O in the oxidation film have a self-diffusion speed, the growth rate of the oxidation film would be rather slow[19]. Cr ions diffuse slowly through the SiO_2 film to the oxidation film surface, then react with oxygen anion to form Cr_2O_3 film, preventing the further oxidation. Therefore, as oxi-

dation time increases, Cr ions diffused to surface are nearly exhausted due to combining with oxygen ions, and the subsequent chromium ions could not be sufficiently supplied. As a consequence, the reaction of iron ions and oxygen ions becomes the main process. Fe_2O_3 film forms above Cr_2O_3 film, and iron ions and oxygen ions diffuse faster in iron oxides than in silicon oxides and chromium oxides. Thus, Fe_2O_3 film thickens quickly. Nevertheless, the oxidation resistance of materials has been degraded to hardly have protection abilities.

As pointed out in previous research, when oxidation occurs in Fe-Cr base alloys, metal and oxygen react quickly, and the metal cations transfer to reaction interface through the oxidation film, or oxygen anions diffuse to reaction interface through the oxidation film as well, so the process of ions transfer to reaction interface through the oxidation film is the controlling step. In conclusion, the diffusion of ions through the oxidation film is the key step of the whole process. Huntz and Bague[20] studied the effect of Si on the high temperature oxidation behaviors of 9%Cr steel and indicated that increasing the amount of Si could reduce the critical amount of chromium required to form integral Cr_2O_3, and the SiO_2 film falls in between Cr_2O_3 film and the substrate, preventing oxygen diffusing into the substrate. In this study, the SiO_2 film exists in the interface of the substrate and the oxidation film, and ions have a low diffusion rate in the SiO_2 film, which delays the oxidation process for the most part, so the oxidation resistance is improved. Moreover, the addition of Si reduces the critical chromium amount, promoting the formation of Cr_2O_3 film on the surface, and the oxidation process is constrained consequently. However, excessive addition of Si could influence the mechanical properties of the material[21], and the plasticity of material reduces when Si content is higher than 1.5% in previous work by author. In this experiment, the Si content of 1.5% would be the optimal.

4. Conclusions

(1) Both the oxidation rate of 30Cr13 stainless steel and the thickness of oxide film will reduce when the amount of Si content increases.

(2) The oxidation surface of Si0.5, Si1.0 and Si1.2 are composed of wheat-like oxides (iron oxide), whereas Si1.5 and Si2.5 are overspread with granulate oxide, and Si1.5 and Si2.5 show better oxidation resistance.

(3) With the addition of Si, a pyknotic silica film that could hinder metal cation spread outward and inward diffusion of oxygen anion on the matrix is formed, which enhances high-temperature oxidation dramatically.

References

[1] P. Zhang, Effect of Heat Treatment Process on Microstructure and Properties of Cr13-type Stainless Steel, Chongqing University, Chongqing, 2005 (in Chinese).
[2] B. He, B. J. Wang, Special Steel (2009) No. 2, 30-33 (in Chinese).
[3] X. Z. Huang, Y. T. Yang, Chin. J. Mater. Res. 28 (2014) 1-9.
[4] H. Fujikawa, T. Morimoto, Y. Nishiyama, Corros. Sci. 59 (2003) 23-40.
[5] T. Morin, M. Rigaud, Can. Metall. Quart. 521 (1970) 4-9.
[6] D. W. Bridges, J. P. Baur, G. S. Baur, W. M. Fassel, J. Electrochem. Soc. 475 (1956) 108-109.
[7] S. Mrowec, A. Stoklosa, Oxid. Met. 291 (1971) 8-9.
[8] D. T. Hoelzer, B. A. Pint, I. G. Wright, J. Nucl. Mater. 1306 (2000) 283-287.
[9] H. T. Wang, Effect and Mechanism of Composite Oxide Scale on Oxidation Resistance of Ferro Based Super Alloys, Shandong University, Jinan, 2010 (in Chinese).
[10] H. E. Evans, D. Hilton, R. Holm, S. Webster, Oxid. Met. 19 (1983) 1-3.
[11] J. Dunning, D. E. Alman, J. C. Rawers, Oxid. Met. 409 (2002) 27-28.
[12] L. Mikkelsen, S. Linderoth, J. B. Sorensen, Mater. Sci. Forum 461 (2004) 117-119.
[13] T. Ishituka, Y. Inoue, H. Ogawa, Oxid. Met. 61 (2003) 124-125.
[14] J. Mougin, M. Dupeux, L. Antoni, A. Galerie, Mater. Sci. Eng. A 12 (2003) 44-51.
[15] M. S. Li, High Temperature Corrosion of Metal, Metallurgical Industry Press, Beijing, 2001 (in Chinese).
[16] Q. H. Zhao, J. Y. Liu, J. Liu, Foundry Technology 32 (2011) 181-183 (in Chinese).
[17] G. Bamba, Y. Wouters, A. Galerie, F. Charlot, A. Dellali, Acta Mater. 54 (2006) 33-39.
[18] N. Birks, G. H. Meier, F. Pettit, Introduction to High Temperature Oxidation of Metals, Press of Higher Education, Beijing, 2010.
[19] T. F. Li, High Temperature Oxidation and Hot Compress of Metal, Press of Chemical Industry, Beijing, 2004 (in Chinese).
[20] A. M. Huntz, V. Bague, Appl. Surf. Sci. 207 (2003) 270-271.
[21] M. Zhou, Study on the Microstructure and Mechanical Properties of the Novel High Silicon Ferritic/martensitic Steels, Nanjing University of Science and Technology, Nanjing, 2013 (in Chinese).